Appl Phys A (2013) 110:269–273
DOI 10.1007/s00339-012-7450-0

Applied Physics A
Materials Science & Processing

RAPID COMMUNICATION

Thermal conductivity enhancement in carbon nanotube/Cu–Ti composites

Ke Chu · Cheng-chang Jia · Wen-sheng Li

Received: 22 August 2012 / Accepted: 16 November 2012 / Published online: 28 November 2012

Abstract Carbon nanotube reinforced Cu–Ti alloy (CNT/Cu–Ti) composites are fabricated by a powder metallurgical method. The interfacial bonding of CNT/Cu–Ti composites is evidently improved, which is attributed to the formation of a thin layer of TiC at the interface. The thermal conductivity of the composites increases by 7.5 % and 15.1 % compared to that of Cu–Ti matrix at CNT loadings of 5 vol.% and 10 vol.%, respectively. The matrix-alloying is therefore an effective way to enhance the thermal conductivity of CNT/Cu composites.

1 Introduction

Carbon nanotubes (CNTs) have great potential applications due to their very large aspect ratio, high rigidity and high tensile strength, excellent electrical conductivity, and thermal conductivity, which make them suitable candidates in preparing composites with newly excellent properties [1]. During the last few years, novel CNT/metal composites have been developed and a number of researchers have reported improved mechanical properties in the case of these composites compared to the pure metals. In an ideal situation, a fully dense composite with a perfect CNTs dispersion throughout metal matrix while avoiding any CNTs damage and agglomeration during processing is required, with the aim of controlling CN/metal performance [2, 3]. A recent comprehensive review [4] discusses the various processing routes developed in order to explore the use of CNTs in metal matrix composites, and summarizes the resulting properties. In addition, Cu matrix composites with a low thermal expansion, high electrical, and thermal conductivity coefficients have been studied for a variety of applications [5], and CNT-reinforced Cu matrix (CNT/Cu) composites are very attractive to meet the increasing demands for high performance thermal management materials used in heat sinks and electronic packages [6–10].

In the case of CNT/Cu composites, it is known there is a very weak bonding between CNT and pure Cu matrix since Cu is known to be naturally nonwetting with CNT [7]. Previous research has indicated that heat transport in a CNT/Cu composite would be limited by the weak interfacial bonding of CNT-Cu, and that the thermal conductivity of the composite would be much lower than the value estimated from the intrinsic thermal conductivity of the nanotubes and their volume fraction [8–11]. In order to solve the interface problem between copper and CNTs, an effective method to improve the interfacial bonding is through the deposition of metal-coating layers on the CNTs [7, 12]. The metal-coating CNTs could efficiently reduce the interface energy mismatch between the copper matrix and the CNTs, therefore, the bonding strength and whole properties of the composites can be improved. Nevertheless, the recent experimental results indicated that the thermal conductivities of the nickel-coated nanotube reinforced copper composite were slightly lower than those of the sintered copper-nickel matrix [12]. The possible reason is that the coating process can introduce additional impurities to the final compact material (e.g., coming from chemicals used in the coating process), which can act as scattering points, resulting in great drop in thermal conductivity. Moreover, the coating layer is easily damaged

K. Chu (✉) · W.-s. Li
State Key Laboratory of Gansu Advanced Non-ferrous Metal Materials, Lanzhou University of Technology, Lanzhou 730050, China
e-mail: chukelut@163.com

C.-c. Jia
School of Material Science and Engineering, University of Science and Technology Beijing, Beijing 100083, China

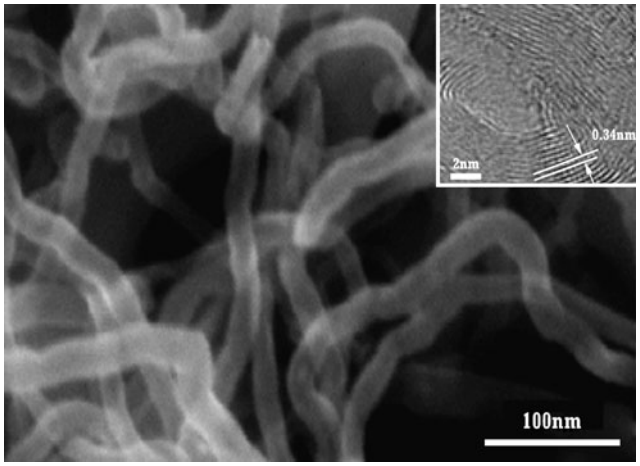

Fig. 1 SEM image of purified CNTs (*inset* for HRTEM image of a section of the wall of one of the nanotubes)

during the subsequent densification processing, which can weaken and even destroy the integration between CNTs and metal matrix and cause a significant degradation in thermal conductivity.

On the other hand, it is well known that alloying of copper with a strong carbide forming element promotes wetting and bonding of carbon materials [13, 14]. However, to-date, there are very few experimental studies focusing on the use of alloying elements added to the copper matrix to modify the interface between the CNTs and copper matrix. The influence of the interface formation on the thermal conductivity of these composites is also not yet fully understood. In this work, we investigate the effect of the titanium applied as a matrix-alloying element on the thermal conductivity of CNT/Cu composites.

2 Experimental

Prealloyed Cu-0.85 wt.% Ti powders with a mean particle size of 15 μm prepared by gas atomization were used as matrix materials. The CNTs used in this study were commercially available as multiwalled CNTs, which were fabricated by the catalytic decomposition of CH_4. The CNTs have an average outer diameter of 10 nm, lengths of up to 15 μm, and a density of 1.7 g/cm^3. The ultrasonic cleaning (in concentrated nitric acid) was performed to remove the impurities in as-received CNTs. It is shown in SEM image (Fig. 1) that the purified CNTs are curled, kinked, and some of them are highly twisted with each other because of the strong intertube van der Waals attraction. The inset of Fig. 1 shows a high-resolution TEM image of a section of the wall of one of the nanotubes, exhibiting the high-quality of nanotube with clearly graphene layers in the wall. The wall interspacing was averaged at 0.34 nm, which is typical of the (002) basal plane of graphite.

Table 1 Thermal conductivity measurements of the composites

Samples	CNT content vol.%	Thermal conductivity W/mK	Relative density %
CNT/Cu	0	325	99.8
	5	321	99.6
	10	318	99.2
CNT/Cu–Ti	0	315	99.7
	5	348	99.3
	10	362	99.0

In order to obtain a high dispersion of CNTs in matrix powders, the CNTs with 5 and 10 vol.% were mixed with Cu–Ti powders by a high-energy ball-milling process at an optimum mixing condition of 1200 revolutions per minute (rpm) in rotary speed and 120 min in duration. The ball-to-powder weight ratio was set to 10:1, and alcohol was added as a process control agent. The compact powders were sintered to disk-shaped samples by hot pressing. The sintering parameters were adjusted to ensure the fully densified microstructure for all samples. The sintering parameters are at 780 °C for 15 min under the uniaxial pressure of 40 MPa. For comparison purposes, the sintered pure Cu and Cu–Ti specimens and the CNT/Cu composites with CNT contents of 5 vol.% and 10 vol.% without Ti addition were also fabricated under the same processing. Density of the samples was measured by the Archimedes method and their theoretical density calculated by the rule of mixtures assuming the densities of 8.96 g/cm^3 for matrix and 1.7 g/cm^3 for CNTs; accordingly, all samples were >99 % of the theoretical density to avoid the influence of the porosity of specimens (Table 1).

The microstructure of the composites was characterized by SEM equipped with energy dispersive X-ray spectroscopy (EDS), and high-resolution transmission electron microscopy (HRTEM). The room temperature thermal diffusivity of the specimens was measured using a transient thermal flash technique. In the measurements, an instantaneous surface heat source was created by a laser pulse absorbed by a sample surface. The thermal wave spread across the sample thickness and emitted a gradually increasing infrared thermal radiation detected by a signal detector with preamplifier. The detector signal was recorded and converted to data information by a data acquisition device, which was directly transmitted to a computer. The specific heat of the specimens was measured using a differential scanning calorimeter with reference materials of single crystal alumina under argon gas. The thermal conductivity of the composites was then calculated as a product of the density, thermal diffusivity and specific heat. The measurements of thermal conductivity are listed in Table 1.

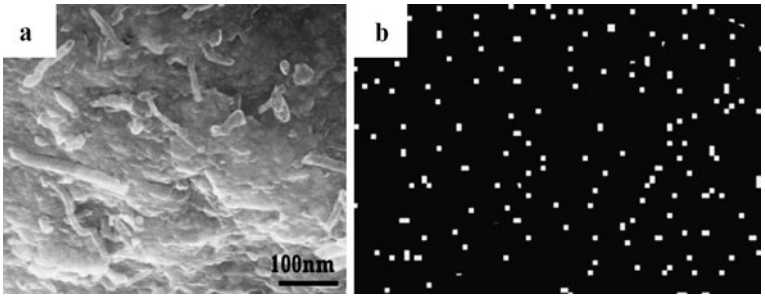

Fig. 2 (**a**) Morphologies of 10 vol.% CNT/Cu–Ti mixed powders and (**b**) EDS mapping profile of 10 vol.% CNT/Cu–Ti composites (C signals)

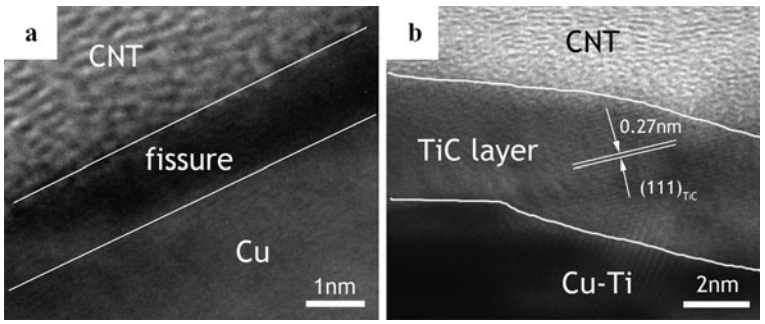

Fig. 3 HRTEM images of the interface in (**a**) CNT/Cu composites and (**b**) CNT/Cu–Ti composites

3 Results and discussion

Figure 2(a) illustrates the uniformly blended Cu–Ti powders and CNTs. It is clearly noticed that the CNTs are mainly residing on the surfaces of the alloy powders, and the CNT agglomerates can not been found in the powder mixtures. Figure 2(b) shows the EDS map parallel to the surface of 10 vol.% CNT/Cu–Ti composite. EDS mapping reveals that the C element is homogeneously mixed in the matrix. This indicates that the combined ball-milling and hot-pressing applied in the present work is effective to achieve the composites with uniform dispersion of the CNTs in the matrix.

HRTEM is utilized to study the interface microstructure of the composites, as shown in Fig. 3. It is evident in Fig. 3(a) that the interface between the pure copper and the CNT is weak, where the clear fissure is observed. It is well known that the determining factor for wetting is surface tension. In general, CNT (carbon) surface tension ranges from 100 to 200 mN/m [15], while Cu surface tension is 1270 mN/m [14, 15]. This means that the Cu matrix will not wet the CNT surface due to the large difference in these surface energies. In addition, Cu is not expected to have any chemical reaction with the CNTs according to the Cu–C phase diagram [16]. Hence, the poor wettability of CNT by copper results in low interface adhesion of this composite system. In contrast, it is obvious in Fig. 3(b) that there is a diffusion TiC reaction layer between CNT and Cu–Ti matrix in CNT/Cu–Ti composites, which can chemically enhance the interfacial bonding.

In Ti–C system, the chemical reactions and the corresponding free energy can be represented by the equations below [17]:

$$\mathrm{Ti} + \mathrm{C} = \mathrm{TiC}, \qquad \Delta G_{\mathrm{TiC}} = \Delta G^{0}_{\mathrm{TiC}} + RT \ln \frac{a_{\mathrm{TiC}}}{a_{\mathrm{Ti}}} \tag{1}$$

where G^0 refers to the standard free energy of formation per mol of carbon, a denotes activity, R the universal gas constant, and T the absolute temperature at which the reaction takes place. The thermodynamic properties of CNTs are assumed equal to graphite due to lack of the data for CNTs. Nonetheless, the Ti–C system might be also accurate for the Ti–CNT system well, because for both graphite and CNT the reacting planes are the same (the (0001) basal and the $(10\bar{1}0)$ prism planes) [18]. Substituting the thermophysical parameters [17, 19], the free energy of formation of TiC (ΔG_{TiC}) at the sintering temperature of 1053 K is obtained as −157.6 kJ/mol, which implies that the above reaction spontaneously progresses during the sintering process. Generally, carbide formation is restricted at the CNT/metal interface due to the absence of a prism plane in CNTs, while these damaged CNTs have broken carbon bonds in the prism planes of outer surface and tips, which would facilitate the formation of carbides in the presence of strong carbide forming element [18, 20]. In the present work, during the ball milling process, CNTs receive impact energy from the balls and this breaks the CNTs and produces the defect sites on the surface of the CNTs. The defects on the CNT walls can also be created by thermal disturbance introduced in the lattice structure, when exposed at reaction temperature. Moreover, the unstable dangling bonds at joints of CNTs are found leading to highly reactive properties. All

of the damaged or defect sites on the surface of CNTs are more prone to reaction-product formation. The formation of TiC on the surface and tips of the CNTs improves the wettability and the interfacial adhesion of CNTs and Cu–Ti matrix.

The experimental thermal conductivities of CNT/Cu–Ti and CNT/Cu composites at 5 vol.% and 10 vol.% loadings are shown in Fig. 4. It confirms that alloying of the copper matrix with the carbide-forming element Ti has a positive effect on the thermal conductivity of the CNT reinforced copper composites. As seen, with 5 vol.% and 10 vol.% CNTs, the thermal conductivities of CNT/Cu–Ti composites increase by 7.5 % and 15.1 %, i.e., to 342 and 366 W/mK from 318 W/mK of Cu–Ti matrix, respectively. Without alloying, the addition of CNTs does not present any enhancement and, on the contrary, slightly reduces the thermal conductivity of CNT/Cu composites.

The conductivity measurements are compared with theoretical predictions, using the model of Nan et al. [21], which includes the effect of interfacial thermal resistance (R_K) and assumes a random distribution of the reinforcing CNTs:

$$\frac{K_e}{K_m} = \frac{3(K_x/K_m + 1) + f[2(K_x/K_m - 1) + (K_x/K_m + 1)(K_z/K_m - 1)]}{3(K_x/K_m + 1) - 2f(K_x/K_m - 1)} \tag{2a}$$

$$K_x = \frac{K_c}{2R_K K_c/d + 1}, \qquad K_z = \frac{K_c}{2R_K K_c/L + 1} \tag{2b}$$

Material properties K_e, K_c, and K_m are the thermal conductivities of the composite, the CNT and the matrix, respectively; K_x and K_z are the effective thermal conductivities of the CNTs along transverse and longitudinal axes, respectively; f is the CNT volume fraction; d and L are the diameter and length of CNT, respectively. In the calculations, the thermal conductivities of Cu–Ti alloy, pure copper and CNT are taken to be 318 W/mK (measured value), 331 W/mK (measured value) and 3,000 W/mK [22], respectively. The average diameter and length of CNTs are 10 nm and 15 μm determined by SEM observations, respectively. Given these parameters, we obtain fits to our data, as shown in Fig. 4, with $R_K = 6.5 \times 10^{-8}$ m^2 K/W for CNT/Cu–Ti composites and $R_K = 8.4 \times 10^{-7}$ m^2 K/W for CNT/Cu composites. This indicates that the interfacial thermal resistance of CNT/Cu composites exceeds that of CNT/Cu–Ti composites by one order of magnitude. Hence, the large interfacial thermal resistance in CNT/Cu composites considerably limits the utility of CNTs for enhancing thermal properties of copper materials and causes the thermal conductivity of the composites even lower than that of copper matrix.

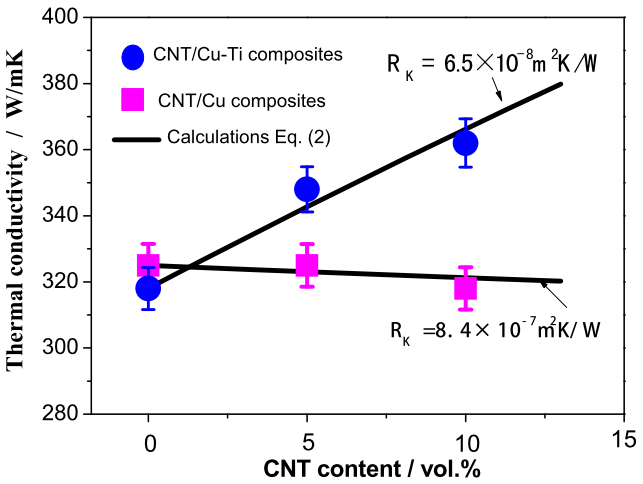

Fig. 4 Thermal conductivity measurements and predictions (Eqs. (2a), (2b)) of CNT/Cu–Ti and CNT/Cu composites versus CNT content

In general, for metal/CNT composites, electrons dominate heat conduction in metals, whereas phonons dominate heat in CNTs. Hence, for heat transport to occur across CNT–metal interfaces, energy transfer must occur between electrons and phonons [23, 24]. Therefore, for the present CNT/Cu composites, the interface scattering of electrons and phonons is higher due to the poor bonding between copper matrix and CNTs, which results in a large interfacial thermal resistance at the CNT–Cu interface, thereby reducing the thermal conductivity of the overall system. Presence of metallurgy bonds between the CNTs and the copper matrix due to the formation of a very thin interface layer of a carbide phase facilitates the necessary electron-phonon coupling and reduces the scattering of electrons and phonons at the interface, in turn improves the thermal conduction in the overall composite.

4 Conclusions

In summary, the Ti applied as a matrix-alloying element is used to improve the interfacial bonding and thermal conductivity of CNT/Cu composites. The microstructure analysis suggests that the high embedding CNTs and strong interfacial bonding can be successfully achieved through the formation of thin TiC layer at the interface. The thermal

conductivity of CNT/Cu–Ti composites is significantly enhanced compared to that of CNT/Cu composites. Our findings would help to understand the effect of interface interaction between CNTs and Cu matrix on the thermal properties of CNT/Cu composites and provide a hint for preparing composites with optimal thermal properties.

Acknowledgements This study was financially supported by National Natural Science Fund of China (No. 51274041) and Doctoral Start-up Scientific Research Fund (2011010431).

References

1. E.T. Thostenson, Z. Ren, T.W. Chou, Compos. Sci. Technol. **61**, 1899 (2001)
2. C. Goh, J. Wei, L. Lee, M. Gupta, Mater. Sci. Eng. A **423**, 153 (2006)
3. K. Chu, C. Jia, L. Jiang, W. Li, Mater. Des. **45**, 407 (2013)
4. S. Bakshi, D. Lahiri, A. Agarwal, Int. Mater. Rev. **55**, 41 (2010)
5. K. Chu, C. Jia, H. Guo, W. Li, Mater. Des. **45**, 36 (2013)
6. K.T. Kim, S.I. Cha, S.H. Hong, Mater. Sci. Eng. A **430**, 27 (2006)
7. W.M. Daoush, B.K. Lim, C.B. Mo, D.H. Nam, S.H. Hong, Mater. Sci. Eng. A **513**, 247 (2009)
8. K. Chu, Q. Wu, C. Jia, X. Liang, J. Nie, W. Tian, G. Gai, H. Guo, Compos. Sci. Technol. **70**, 298 (2010)
9. K. Chu, H. Guo, C. Jia, F. Yin, X. Zhang, X. Liang, H. Chen, Nanoscale Res. Lett. **5**, 868 (2010)
10. S. Cho, K. Kikuchi, A. Kawasaki, Acta Mater. **60**, 726 (2012)
11. K. Chu, W. Li, H. Dong, F. Tang, Europhys. Lett. **100**, 36001 (2012)
12. C. Kim, B. Lim, B. Kim, U. Shim, S. Oh, B. Sung, J. Choi, J. Ki, S. Baik, Synth. Met. **159**, 424 (2009)
13. J. Silvain, D. Coupard, Y. Le Petitcorps, M. Lahaye, M. Onillon, X. Goni, J. Mater. Chem. **10**, 2213 (2000)
14. B. Dewar, M. Nicholas, P. Scott, J. Mater. Sci. **11**, 1083 (1976)
15. D. Mortimer, M. Nicholas, J. Mater. Sci. **5**, 149 (1970)
16. S. Datta, S.N. Tewari, J.E. Gatica, W. Shih, L. Bentsen, Metall. Mater. Trans. A, Phys. Metall. Mater. Sci. **30**, 175 (1999)
17. P. Kollman, Chem. Rev. **93**, 2395 (1993)
18. L. Ci, Z. Ryu, N.Y. Jin-Phillipp, M. Rühle, Acta Mater. **54**, 5367 (2006)
19. A. Steinfeld, Sol. Energy **78**, 603 (2005)
20. T. Laha, S. Kuchibhatla, S. Seal, W. Li, A. Agarwal, Acta Mater. **55**, 1059 (2007)
21. C.W. Nan, R. Birringer, D.R. Clarke, H. Gleiter, J. Appl. Phys. **81**, 6692 (1997)
22. P. Kim, L. Shi, A. Majumdar, P. McEuen, Phys. Rev. Lett. **87**, 215502 (2001)
23. A. Majumdar, P. Reddy, Appl. Phys. Lett. **84**, 4768 (2004)
24. K. Chu, C. Jia, W. Li, Appl. Phys. Lett. **101**, 121916 (2012)